HHS Public Access

Author manuscript

Mol Cancer Res. Author manuscript; available in PMC 2019 December 17.

Published in final edited form as:

Mol Cancer Res. 2019 March ; 17(3): 741–750. doi:10.1158/1541-7786.MCR-18-0451.

Ovarian Tumor Cell Expression of Claudin-4 Reduces Apoptotic Response to Paclitaxel

Christopher Breed[1,2], **Douglas A. Hicks**[1], **Patricia G. Webb**[1], **Carly E. Galimanis**[1], **Benjamin G. Bitler**[1], **Kian Behbakht**[1,2], **Heidi K. Baumgartner**[1,2]

[1]Divisions of Reproductive Sciences, University of Colorado Denver, Anschutz Medical Campus, 12700 E. 19th Avenue, Aurora, Colorado, 80045 USA

[2]Gynecologic Oncology, Department of Obstetrics and Gynecology, University of Colorado Denver, Anschutz Medical Campus, 12700 E. 19th Avenue, Aurora, Colorado, 80045 USA

Abstract

A significant factor contributing to poor survival rates for ovarian cancer patients is insensitivity of tumors to standard-of-care chemotherapy. In this study, we investigated the effect of claudin-4 expression on ovarian tumor cell apoptotic response to cisplatin and paclitaxel. We manipulated claudin-4 gene expression by silencing expression (shRNA) in cells with endogenously expressed claudin-4 or overexpressing claudin-4 in cells that natively do not express claudin-4. Additionally, we inhibited claudin-4 activity with a claudin mimic peptide (CMP). We monitored apoptotic response by caspase-3 and Annexin V binding. We examined proliferation rate by counting cell number over time as well as measuring number of mitotic cells. Proximity ligation assays, immunoprecipitation, and immunofluorescence were performed to examine interactions of claudin-4. Western blot analysis of tubulin in cell fractions was used to determine changes in tubulin polymerization with changes in claudin-4 expression. Results show that claudin-4 expression reduced epithelial ovarian cancer (EOC) cell apoptotic response to paclitaxel. EOCs without claudin-4 proliferated more slowly with enhanced mitotic arrest compared to cells expressing claudin-4. Furthermore, our results indicate that claudin-4 interacts with tubulin, having a profound effect on the structure and polymerization of the microtubule network. In conclusion, we demonstrate that claudin-4 reduces ovarian tumor cell response to microtubule-targeting paclitaxel and disrupting claudin-4 with CMP can restore apoptotic response. Implications: These results suggest that claudin-4 expression may provide a biomarker for paclitaxel response and can be a target for new therapeutic strategies to improve response.

INTRODUCTION

Due to the lack of adequate early detection screening, the majority (> 85%) of patients with epithelial ovarian cancer (EOC) are diagnosed at advanced stages of disease. Delayed detection means that ovarian tumor cells have disseminated beyond their site of origin

Corresponding Author: Heidi K. Baumgartner Wilson, Ph.D., Assistant Professor, Department of Obstetrics and Gynecology, Division of Reproductive Sciences, University of Colorado Denver Anschutz Medical Campus, Mail Stop 8613, 12700 E. 19th Ave., Aurora, CO 80045, Heidi.Wilson@ucdenver.edu, Phone: 303-724-3505, Fax: 303-724-3512.

Conflict of Interest Statement: All authors declare no conflicts of interest.

(fallopian tube or ovary) into the peritoneal cavity. The standard of care for these patients is surgical debulking of the tumor followed by adjuvant platinum- and taxane- based chemotherapies (cisplatin/carboplatin and paclitaxel/docetaxel) [1]. One third of ovarian cancer patients have tumors that do not respond to initial chemotherapy and of the patients that do respond, approximately 75% of these patients will have disease recurrence [2]. Patients with recurrent EOC succumb to the disease following development of chemoresistance [3].

There are several proposed mechanisms responsible for reduced therapeutic response that include both *de novo* pathways that inherently make tumor cells resistant and acquired pathways that are upregulated in response to repeated chemotherapeutic insult. These pathways include, but are not limited to: drug transporters (i.e. P-glycoprotein) that either inhibit drug uptake or enhance drug efflux [4–6], epigenetic changes (i.e. MLH1 and Tap73 methylation, miR-214 and miR-376c upregulation) that prevent expression of anti-tumorigenic genes [7–10], expression or mutations in pro-apoptotic proteins (i.e. p53, Bcl-2 family proteins, PTEN [11–14]), and cytoskeletal organization that prevents binding of microtubule-targeting agents [15]. Despite the increased understanding of chemoresistance mechanisms, it is unlikely that a single pathway can be targeted to restore tumor sensitivity to all cytotoxic drugs. However, a deeper understanding of patient genetic and proteomic characteristics that can predict response and inform optimal therapeutic strategies is a significant step forward.

Claudin-4 is a member of a large family of transmembrane proteins, of which there are 27 different subtypes [16]. Claudins have been most studied for their canonical role in tight junctions, where they mediate the specific paracellular barrier properties of an epithelium. Although claudin-4 has been shown to alter the permeability of epithelial monolayers in cell culture [17–19], it is rarely localized to tight junctions in human and mouse tissue and is generally found along basolateral membranes and throughout the cytosol [20–22]. The findings that claudin-4 knockout (KO) mice are phenotypically normal with only a subclinical increase in permeability to small molecules in lung epithelium but have a reduced capacity for wound healing, further suggest a non-canonical role for claudin-4 [23]. Furthermore, it has been well documented that claudin-4 is significantly upregulated in multiple epithelia-derived cancer cells that lack traditional tight junction structures. High claudin-4 expression has, in fact, been associated with a phenotypically aggressive ovarian cancer cell (chemoresistant, highly mobile, and stem-like [24–26]). The mechanism by which claudin-4 exerts these effects is currently unknown.

To investigate the non-canonical role of claudin-4 in both normal and tumor cell biology, we previously designed a small claudin mimic peptide (CMP) that interferes with the DFYNP sequence in the second extracellular loop of claudin-4 that is thought to be important in claudin-claudin interactions [27]. We have recently shown that disrupting claudin-4 activity with CMP increased tumor cell response to the potent apoptotic inducer staurosporine and inhibited cell migration [28]. Additionally, treatment of mice bearing EOC cell line-derived xenograft tumors with CMP significantly reduced tumor burden. These observations suggest that claudin-4 expression in ovarian cancer cells plays a functional role in tumor progression.

To determine whether claudin-4 plays a role in the apoptotic response of ovarian tumors to standard chemotherapeutics, we examined whether the presence of the protein altered the apoptotic response of EOC cell lines to cisplatin and paclitaxel in the presence and absence of CMP. We found that claudin-4 expression led to reduced tumor cell sensitivity to paclitaxel-induced apoptosis. Tumor cell sensitivity to paclitaxel was restored by silencing claudin-4 expression or co-treatment with CMP. We also show claudin-4 involvement in cell cycle progression and an interaction of claudin-4 with microtubules, providing a possible mechanism by which claudin-4 drives resistance to paclitaxel.

MATERIALS AND METHODS

Cell culture:

Human-derived OVCAR3, OVCAR4, OVCAR5, OVCAR8, PEO4, OV429, and DOV13 ovarian tumor cells were obtained from the laboratory of Monique A. Spillman (University of Colorado Denver, Aurora Colorado) and cultured in RPMI-1640 medium (Gibco, Thermo Fisher Scientific, Grand Island, NY, USA) plus 10% heat-inactivated fetal bovine serum (Access Cell Culture, Vista, CA, USA) and 1% penicillin/streptomycin (Gibco, Thermo Fisher Scientific) at 37°C and 5% CO_2. Cells were trypsinized (0.25% trypsin, EDTA, Mediatech) and plated 1:3 every 3–4 days. All cell lines were authenticated at the beginning of this study by short tandem repeat profiling, as described previously [29]. Cells were passaged approximately 10 times before thawing out a fresh vial of authenticated cells. Authentication was then repeated at the end of the study. Cells were plated at 1×10^4 cells/well into type I collagencoated 8-well chamber slides (Lab-Tek, NUNC, Rochester, NY, USA) for treatment and analysis. Upon 80–90% confluence, cells were treated with either 400 μM control peptide (NH2GDGYNPG-OH, D-amino acid conformation, University of Colorado Protein and Peptide Chemistry Core [27]), 400 μM claudin mimic peptide (CMP, NH2-GDFYNPG-OH, D-amino acid conformation, University of Colorado Protein and Peptide Core), 10 nM paclitaxel (SigmaAldrich, St Louis, MO, USA), and/or 10 μM cisplatin (Sigma-Aldrich) for 24 hours. To examine the apoptotic mechanism, cells were also treated with 50 μM etoposide (Sigma-Aldrich).

Ovarian Tumor Samples:

De-identified patient tumor samples were collected from the University of Colorado Gynecologic Tissue and Fluid Bank under an Institutional Review Board approved protocol (COMIRB 05–1081). Each tumor sample was flash frozen in liquid nitrogen and stored at −80°C until processed for protein. Frozen tissue was placed in lysis buffer (30 mM Tris HCl pH7.4, 150 mM NaCl, 1% TritonX-100, 10% glycerol, 2 mM EDTA, 0.57 mM PMSF, 1X cOmplete™ Protease Inhibitor Cocktail) and homogenized using a Polytron tissue homogenizer (Brinkmann Instruments, Fisher Scientific). Lysates were then spun at 13,000 rpm for 10 minutes and the supernatant collected for protein analysis.

Western blot analysis:

To determine levels of claudin-4 protein expression, tumor cells were scraped from culture plates in presence of lysis buffer (30 mM Tris HCl pH7.4, 150 mM NaCl, 1% TritonX-100, 10% glycerol, 2 mM EDTA, 0.57 mM PMSF, 1X cOmplete™ Protease Inhibitor Cocktail),

placed on a shaker for 10 minutes and spun at 13,000 rpm for 10 minutes. Supernatant was collected and 20 ug of total protein was denatured, resolved on 10% SDSPAGE, and transferred to a polyvinylidene difluoride (PVDF) membrane (Bio Rad, Hercules, CA, USA). Membranes were blocked with 5% nonfat dry milk in Tris-buffered saline with 0.1% Tween-20 (TBST) for one hour at room temperature (RT) before treatment with either rabbit anti-human claudin-4 (1:500, Invitrogen), mouse anti-human claudin-4 (1:500; Invitrogen), or rabbit anti-human GAPDH (1:10,000; Sigma) overnight at 4°C. Membranes were then washed 4 times with TBST for 15 minutes before treatment with horseradish peroxidase-conjugated goat anti-rabbit (1:10,000; GE Healthcare, Buckinghamshire, UK) or goat anti-mouse (1:10,000; Jackson ImmunoResearch Laboratories, West Grove, PA, USA) antibodies for 1 hour at room temperature. Membranes were washed with TBST as described above and then visualized using an ECL Prime Western Blotting Detection Reagent (GE Healthcare) and X-ray film (CLXPosure Film, Thermo Scientific, Rockford, IL, USA).

Caspase activation assay:

Apoptosis was measured by determining the number of cells exhibiting activated caspase-3. After treatment, cells were washed with phosphate buffered saline (PBS; Gibco, Thermo Fisher Scientific) and fixed with 10% phosphate buffered formalin (Fisher Scientific, Pittsburg, PA, USA) at room temperature (RT) for 15 minutes. Cells were washed twice with PBS before cell membrane permeablization with 0.5% Triton X-100 (IBI Scientific, Peosta, IA, USA) for 5 minutes and washed again with PBS. Cells were treated with blocking buffer (2% bovine serum albumin; Sigma-Aldrich) for 1 hour before application of primary antibody directed to cleaved caspase-3 (1:400; rabbit anti-human cleaved caspase-3, Cell Signaling, Danvers, MA, USA) overnight at 4°C. Cells were then washed with PBS five times before application of secondary antibody conjugated to CY3 (1:100; donkey anti-rabbit, Jackson ImmunoResearch Laboratories, West Grove, PA, USA) and 5 μg/ml 4’,6-diamidina-2phenylindole (DAPI; Sigma) for 45 minutes at RT followed by five washings with PBS. After removal of PBS, o-phenylenediamine dihydrochloride (20 mg/ml; OPDA) in 1M Tris, pH 8.5 was added to the slides to preserve fluorescence and coverslipped. The Olympus FV1000/RICS confocal microscope (University of Colorado AMC Light Microscopy Core) was used to image fluorescence. The percent of cells positive for active caspase was determined using SlideBook software (Intelligent Imaging Innovations, Inc., Denver, CO, USA).

shRNA knockdown:

OVCAR3 and PEO4 cells were plated 3.2 ×104 in a 96-well plate and incubated at 37°C for 24 hours. When cells reached 70% confluence, 10 μl of claudin-4 shRNA (TRC#: TRCN0000116627, TRCN0000116628 or TRCN0000116631) or control shRNA (SHC001, pLK0.1-puro Empty Vector) lentiviral suspension (Sigma-Aldrich MISSION® shRNA, University of Colorado Functional Genomics Facility, Aurora, CO, USA) was added to the cells and incubated overnight at 37°C. Fresh medium was added to remove lentivirus and cells were allowed to recover for 24 hours before being treated with 0.5 μg/ml puromycin for selection and expansion of transduced cells. Western blot analysis (as described above) confirmed loss of claudin-4 expression.

Overexpression of claudin-4:

GFP-tagged claudin-4 and a GFP only control (pLenti-C-mGFP vector; OriGene, Rockville, MD, USA) were transduced into OVCAR8 and OVCAR4 cells via lentiviral particles in the presence of 10 μg/ml hexadimethrine bromide. GFP-positive cells were flow sorted and expanded.

Mitotic Assays:

To examine the number of cells in mitosis, we examined images of DAPI fluorescence in OVCAR3 cells cultured in 8-well chamber slides. Cells that had clearly condensed chromatin that aligned along a single plane were counted as mitotic cells and calculated the percentage of total number of nuclei per field of view. (At least 12 fields of view were analyzed for each condition.) Additionally, a Mitotic Assay Kit (Active Motif, Carlsbad, CA, USA) was used per manufacturer's instructions. Briefly, cells were cultured in 96-well plates, fixed, and treated with a phospho-histone H3 (Ser 28) monoclonal primary antibody followed by an HRP-conjugated secondary antibody. Absorbance at 450 nm was read after 20 minute incubation with the Developing Solution. Crystal Violet was used to normalize for total cell number.

Proliferation Assay:

Ten thousand cells were plated in each well of 12-well culture plates. Cells were trypsinized (0.25% trypsin, EDTA) and counted by a Countess™ Automated Cell Counter (Invitrogen) after 24, 48, and 72 hours in culture.

Cell Cycle Analysis:

Cells were plated in 100mm culture dishes at 5×10^5 cells per dish. After 24 hours in culture, media was changed to serum-free RPMI-1640 for 48 hours. Cells were then exposed to media containing serum and harvested 6 hours later. Cells were placed in Krishan Stain (0.224 g NaCitrate $2H_2O$, 9.22 mg propidium iodide, 2.0 mL 1% NP40 in H_2O, 2.0 mL 1 mg/mL RNase in 200 mL H_20) overnight at 4°C before being send to the University of Colorado Flow Cytometry Core Facility. Cells were analyzed by flow cytometry (Beckman Coulter Gallios, University of Colorado Flow Cytometry Core Facility), measuring fluorescence emission at >575 nm (FL3). FlowJo® software was used to determine number of cells in G2/M.

Proximity Ligation Assay:

Claudin-4 interaction with tubulin was examined using DuoLink® Proximity Ligation Assay Kit (Sigma), following manufacturer's protocol. Briefly, cells were plated in 8-well chamber slides and cultured to 70% confluence before being fixed, permeablized, and blocked as described above for capase-3 immunofluorescence. Cells were then treated with antibodies directed to claudin-4 (mouse anti-human claudin-4; 1:200; Invitrogen) and α-tubulin (rabbit anti-human α-tubulin; 1:100; Abcam, Cambridge, MA, USA) or β-tubulin (rabbit anti-human β-tubulin; 1:100; Abcam) overnight at 4°C. After washing with PBS, cells were treated with PLA Probes (1:5; anti-mouse PLUS, anti-rabbit MINUS) for 1 hour at 37°C in a pre-heated humidity chamber. After washing, Ligation Solution was added for 30 min at

37°C followed by washing and addition of Amplification-Polymerase Solution for 100 min at 37°C in a humidity chamber. Slides were washed and dried before adding mounting medium and placing coverslip. Fluorescence was imaged using an Olympus FV1000/RICS confocal microscope (University of Colorado AMC Light Microscopy Core).

Immunoprecipitation:

Claudin-4 (and interacting proteins) was pulled from cell lysates with an antibody directed to claudin-4 (mouse anti-human claudin-4, Invitrogen) bound to Protein A/G Dynabeads® Magnetic beads, using the Pierce™ Crosslink IP Kit (ThermoFisher). Beads were incubated with lysate (~500 μg protein) for 1 hour at room temperature and then collected using a Magnetic Separation Rack (New England BioLabs, Ipswich, MA, USA). Proteins were eluted from beads per manufacturer's protocol. Eluted proteins were run on 10% SDS-PAGE and Western blot analysis was performed as described above, using antibodies directed to claudin-4 (rabbit anti-human claudin-4; 1:500) and tubulin (rabbit anti-human α-tubulin or β-tubulin; 1:1000).

Visualization of claudin-4 and microtubules:

Immunofluorescence was performed, as described above for caspase-3 activation, to visualize claudin-4 and tubulin in tumor cells. Primary antibodies used in these assays were the same (including dilutions) as those described above for the proximity ligation assays.

Tubulin Polymerization Assay:

The Microtubules/Tubulin In Vivo Assay Kit (Cytoskeleton Inc., Denver, Colorado, USA) was used to determine changes in tubulin polymerization with changes in claudin-4 expression. Cells were grown to 80% confluence before being washed with PBS and scraped from 100 cm^2 plates in tubulin stabilization buffer provided by kit manufacturer and homogenized by pipetting. Cell suspension was centrifuged at 1,000 g (37°C) for 5 minutes. Cell pellet and supernatant were collected separately and resolved on 10% SDS-PAGE gel. Primary tubulin antibody and HRP-conjugated secondary antibody provided by kit manufacturer were used to determine polymerized (pellet fraction) and non-polymerized (supernatant fraction) tubulin levels. Densitometry, using ImageJ, was performed to quantify changes in levels of polymerized to non-polymerized tubulin in each cell line.

Statistics:

Data are presented as mean ± standard error of the mean (s.e.m.). An unpaired Student *t* test was used for statistical comparison between control and treatment groups. A oneway ANOVA was used to determine variance among multiple groups, with a Bonferroni Multiple Comparison post-test to determine significance between individual groups. A p value of < 0.05 was considered significant.

RESULTS

Claudin-4 is highly expressed in high grade serous epithelial ovarian tumor cells.

To identify changes in claudin-4 mRNA expression levels in human ovarian cancer patient tumors compared to normal human ovarian surface epithelium, we queried the Gene Expression Ominbus (GEO) database. We analyzed expression in the GSE18521 (ID: 200018521) dataset containing 10 normal human ovarian surface epithelium (HOSE) and 53 high grade serous epithelial ovarian cancer (HGSOC) samples. We found a significant (p = 0.0002) difference in claudin-4 (CLDN4) expression, with 1.8- to 18-fold higher expression in the HGSOC compared to HOSE (Figure 1A). Next, we examined claudin-4 protein expression in patient fallopian tube and tumor samples from the University of Colorado Gynecologic Tissue and Fluid Bank (Figure 1B). The majority of the HGSOC tumor samples expressed claudin-4. In fact, the HGSOC samples expressed significantly (p= 0.0210) more claudin-4 protein than the normal fallopian tube tissue (see Supplementary Data, Figure, 1 for representative Western blots and list of tissue types analyzed). We then examined claudin-4 protein levels in several ovarian tumor cell lines previously identified as having origins from high grade serous epithelial ovarian tumors [29, 30]. In agreement with previous findings, we found that OVCAR3, PEO4, OV429, and OVCAR5 expressed high levels of claudin-4 protein and OVCAR8, OVCAR4, HEY, and DOV-13 cells expressed very low/no claudin-4 protein (Figure 1C).

Claudin-4-expressing cells exhibit a reduced apoptotic response to paclitaxel.

To determine whether the presence of claudin-4 in tumor cells alters the response to standardof-care chemotherapies, we examined activation of caspase-3 in response to cisplatin and paclitaxel. Claudin-4 expressing OVCAR3 cells exhibited an increase in apoptosis (as measured by percent cleaved caspase-3 positive cells) in response to the claudin-4-disrupting peptide (CMP), cisplatin, and paclitaxel individually (Figure 2A&B). Combined treatment with cisplatin and CMP did not enhance cisplatin response (p = 0.3602). However, apoptosis was enhanced nearly 3-fold when cells were co-treated with CMP and paclitaxel compared to paclitaxel alone (p = 0.0002). Similar responses to paclitaxel and CMP were seen in claudin-4expressing PEO4, OV429, and OVCAR5 cells (Supplementary Data, Figure 2A–C). In contrast, the OVCAR8 (lacking claudin-4 expression) cells were more sensitive to both cisplatin (p = 0.0032) and paclitaxel (p = 0.0063) compared to OVCAR3 cells and CMP did not enhance the apoptotic response to either cisplatin or paclitaxel (Figure 2C). Analysis of additional claudin-4 deficient EOC cell lines (OVCAR4 and DOV-13, Supplementary Data, Figure 2D&E) consistently showed no enhancement of the apoptotic response to paclitaxel with CMP co-treatment. As a secondary assay of apoptotic response, we used flow cytometry to measure number of OVCAR3 cells exhibiting Annexin V binding and confirmed enhanced apoptosis (Annexin V binding) in response to paclitaxel when co-treated with CMP (Supplementary Data, Figure 3).

Loss of claudin-4 expression improves tumor cell apoptotic response to paclitaxel.

Using a small-hairpin RNA (shRNA) specific to claudin-4, we knocked down claudin-4 expression in OVCAR3 cells (“shCLDN4_2” and shCLDN4_3, Figure 3A). A control, empty vector, shRNA and shCLDN4_1 did not impact expression of the claudin-4 protein

("shCTRL" and "shCLDN4_1", respectively). Similar to parental OVCAR3 cells, shCTRL and shCLDN4_1 cells showed increased apoptosis with CMP or paclitaxel alone and a significantly enhanced apoptotic response to paclitaxel in the presence of CMP (p <0.0001, Figure 3B). CMP did not induce an apoptotic response in OVCAR3 shCLDN4_2 and shCLDN4_3 cells (cells that successfully lost claudin-4 expression) and CMP co-treatment did not enhance paclitaxel-induced apoptosis (p = 0.8890 and 0.8851, respectively, for shCLDN4_2; p = 0.5024 and 0.7734, respectively, for shCLDN4_3). However, the response to paclitaxel alone was significantly (p <0.0001) higher in the shCLDN4_2 and shCLDN4_3 cells compared to shCTRL and shCLDN4_1 cells, indicating that disrupting claudin-4 augments apoptotic response to paclitaxel. Similar results were seen in the claudin-4 expressing PEO4 cell line (Supplementary Data, Figure 4). (Supplementary Data, Figure 5 shows representative images of nuclei and activated caspase-3 in claudin-4-expressing control and claudin-4 silenced tumor cells.)

Overexpression of claudin-4 reduces tumor cell response to paclitaxel.

We next evaluated the impact of overexpressing claudin-4 in OVCAR8 and OVCAR4 cells which endogenously express no/low claudin-4 protein (Figure 1). We transfected both cell lines with GFP-tagged claudin-4 or a control GFP vector. Western blot analysis showed strong expression of the claudin-4-GFP (Figure 4A). GFP control cells did not respond to CMP treatment; apoptosis was not induced with CMP and paclitaxel apoptotic response was not enhanced with CMP co-treatment. However, cells with claudin-4-GFP overexpression had a decreased apoptotic response to paclitaxel and were responsive to CMP, with induction of apoptosis with CMP alone and enhanced apoptotic response to paclitaxel in the presence of CMP (Figure 4B, representative images of nuclei and activated caspase-3 in claudin-4 non-expressing control and claudin-4 overexpressing tumor cells are shown in Supplementary Data, Figure 6). Similar responses were seen in OVCAR4 cells (Supplementary Data, Figure 7).

Claudin-4 expression results in increased mitotic fidelity.

We have shown in the experiments above that claudin-4 diminishes the apoptotic response to paclitaxel. We next wanted to determine a potential mechanism by which claudin-4 could affect cell biology to influence paclitaxel response. Upon examination of nuclei in the OVCAR3 cell line we observed significantly more mitotic figures in shCLDN4_2 cells compared to the claudin-4 expressing shCTRL cells (p <0.0001, Figure 5A&B). To confirm this observation we used a colorimetric mitotic assay kit that utilizes a phospho-histone H3 (Ser28) monoclonal antibody with HRP-conjugated secondary antibody to detect the level of mitosis. The loss of claudin-4 expression significantly increased the number of cells in the M phase of mitosis (Figure 5C, p <0.0001). To determine whether this increased mitotic index resulted in an increase in cell proliferation, we measured cell number over time in shCTRL and shCLDN4_2 cell lines. We found that the claudin-4 knockdown cells proliferated significantly more slowly than the control cells (p = 0.0453, Figure 5D). Cell cycle analysis, using flow cytometry (Figure 5E&F), confirmed significantly (p = <0.0001) more tumor cells in the G2/M phase at 6 hours post release from serum-free conditions in cells that did not express claudin-4 (shCLDN4_2) compared to cells that did express claudin-4 (shCTRL). These findings suggest that the increase in mitotic figures in the cells

lacking claudin-4 expression is not the result of increased proliferation, but reflects an inhibition of G2/M progression.

Microtubules are known to play an important role in both paclitaxel response and cell cycle progression. Therefore, we examined whether claudin-4 interacted with microtubules. Proximity ligation assays were performed on OVCAR3 cells with antibodies directed to claudin-4 and either α-tubulin or β-tubulin. Claudin-4 was found to be within interacting distance of both α-tubulin and β-tubulin (Figure 6A). Immunoprecipitation (IP) of claudin-4 confirmed interaction with α-tubulin (Figure 6B), but we were unable to confirm interaction with β-tubulin by this method. However, immunofluorescence assays revealed that claudin-4 was co-localized with βtubulin at the mitotic spindle in tumor cells undergoing mitosis (Figure 6C). Additionally, images of microtubules in claudin-4 expressing (shCTRL cells) and non-expressing (shCLDN4_2) OVCAR3 cells revealed significant changes in microtubule structure when claudin-4 expression was present (Figure 6D).

Claudin-4 expression alters polymerization of tubulin.

To identify a potential role for claudin-4 in altering microtubule stability, we examined levels of tubulin within microtubules (polymerized tubulin) compared to free tubulin (non-polymerized tubulin) in OVCAR3 cells expressing and not expressing claudin-4. Figure 7A shows a shift between polymerized (pellet: p) and non-polymerized (supernatant: s) tubulin levels when claudin-4 expression is silenced. Densitometry analysis revealed that there was a significant ($p = 0.0054$) decrease in the percentage of total tubulin found within microtubules (polymerized) in the claudin-4 knockdown (shCLDN4_2) compared to claudin-4 expressing control (shCTRL) cells (Figure 7B), suggesting that claudin-4 is enhancing the polymerization of microtubules.

DISCUSSION

In this study, we have shown that claudin-4 expression reduces the apoptotic response of ovarian tumor cells to paclitaxel. Disruption of claudin-4 expression (shRNA knockdown) or activity (CMP treatment) can enhance or restore the paclitaxel apoptotic response through activation of apoptosis. Additionally, we demonstrated that loss of claudin-4 delayed progression through the cell cycle and reduced proliferation. The effect on both apoptosis and the proliferative response in tumor cells may be due the interaction of claudin-4 with microtubules and alteration of tubulin polymerization.

Previously, high claudin-4 expression was shown to be associated with ovarian tumor cells that are resistant to chemotherapeutic agents [24, 25, 31]. For example, CD44+ ovarian tumor cells were shown to have significantly higher expression levels of claudin-4 compared to CD44- populations isolated from the same tumor. The CD44+/high claudin-4 expressing cells were more resistant to carboplatin and paclitaxel treatment compared to the low/no expressing cells [25]. Additionally, Gao et al. have demonstrated that inhibiting claudin-3 and −4 expression with a fragment of the *Clostridium perfringens* enterotoxin increased ovarian tumor cell response to both paclitaxel and carboplatin [31]. Although our data shows that cells expressing high levels of claudin-4 (OVCAR3) are more resistant to cisplatin compared to cells that do not express claudin-4 (OVCAR8), CMP was unable to enhance the

apoptotic response to cisplatin in the claudin-4 expressing tumor cells. These results suggest the possibility that claudin-4 may regulate the apoptotic response to cisplatin through a different mechanism than paclitaxel, potentially through an interaction of claudin-4 that does not involve the second extracellular loop (which is targeted by CMP).

Previous studies investigating a role for claudin-4 in proliferation have not been consistent. Agarwal et al. demonstrated that overexpressing claudin-4 in normal human ovarian surface epithelial (HOSE) cells enhanced survival, but did not alter proliferation [32]. On the other hand, Ma et al. demonstrated that loss of claudin-4 expression inhibits proliferation in MCF7 breast cancer cells *in vitro* and *in vivo* [33]. The discrepancies could be due to differences in the regulation (or loss of regulation) of claudin-4 in normal versus tumor cells. Additionally, our results demonstrate that tumor cells still proliferate in the absence of claudin-4. This suggests that claudin-4 is not required for proliferation but does enhance proliferation when it is present. The observation that loss of claudin-4 leads to increased number of cells in mitosis indicates that claudin-4 likely enhances proliferation by facilitating progression through mitosis.

A proteomic analysis of proteins within interacting distance of claudin-4 in MDCK cells was performed by Fredricksson et al. and β tubulin was identified as a potential interacting partner of claudin-4 [34]. Our results confirm an interaction of claudin-4 with both α-tubulin and β-tubulin in ovarian tumor cells and that this interaction changes during the cell cycle. We were able to capture an interaction of claudin-4 at sites at or near the plasma membrane as well as within the mitotic spindle. Further analysis of this interaction will be needed to fully understand how interaction of claudin-4 with microtubules may be regulating tumor cell survival and growth. Our results do suggest that interaction of claudin-4 with tubulin may alter the polymerization of tubulin. McGrail and colleagues have shown that ovarian tumor cells that are resistant to paclitaxel-induced death have altered microtubule stability [35]. Therefore, it is possible that claudin-4 alters microtubule dynamics in a way that makes tumor cells more resistant to paclitaxel-induced death.

In conclusion, we have demonstrated that claudin-4 plays an important role in tumor cell resistance to paclitaxel. Therefore, expression of claudin-4 by tumor cells may be a biomarker for patient response to paclitaxel. Additionally, the development of a claudin-4 therapeutic (e.g. CMP) could provide a novel way to improve patient response to paclitaxel.

Supplementary Material

Refer to Web version on PubMed Central for supplementary material.

ACKNOWLEDGEMENTS

The authors wish to acknowledge Dziuleta Cepeniene of the Peptide and Protein Chemistry Core at the University of Colorado for synthesizing CMP. We would also like to acknowledge that imaging was made possible by the University of Colorado Advanced Light Microscopy Core, supported in part by NIH/NCRR CCTSI grant UL1 RR025780. Flow cytometry was performed by the University of Colorado Cancer Center Flow Cytometry Shared Resource (supported by NCI Cancer Center Support Grant P30CA046934). Funding was also provided by the Department of Obstetrics and Gynecology, University of Colorado Denver.

REFERENCES

1. Colombo N, Peiretti M, Parma G, Lapresa M, Mancari R, Carinelli S, Sessa C, Castiglione M: Newly diagnosed and relapsed epithelial ovarian carcinoma: ESMO Clinical Practice Guidelines for diagnosis, treatment and follow-up. Ann Oncol, 21 Suppl 5:v23–30. [PubMed: 20555088]
2. Agarwal R, Kaye SB: Ovarian cancer: strategies for overcoming resistance to chemotherapy. Nat Rev Cancer 2003, 3(7):502–516. [PubMed: 12835670]
3. Muggia FM, Jeffers S, Muderspach L, Roman L, Rosales R, Groshen S, Safra T, Morrow CP: Phase I/II study of intraperitoneal floxuridine and platinums (cisplatin and/or carboplatin). Gynecol Oncol 1997, 66(2):290–294. [PubMed: 9264578]
4. Kavallaris M, Leary JA, Barrett JA, Friedlander ML: MDR1 and multidrug resistanceassociated protein (MRP) gene expression in epithelial ovarian tumors. Cancer Lett 1996, 102(1–2):7–16. [PubMed: 8603381]
5. Zajchowski DA, Karlan BY, Shawver LK: Treatment-related protein biomarker expression differs between primary and recurrent ovarian carcinomas. Molecular cancer therapeutics 2012, 11(2):492–502. [PubMed: 22203729]
6. Svoboda M, Wlcek K, Taferner B, Hering S, Stieger B, Tong D, Zeillinger R, Thalhammer T, Jager W: Expression of organic anion-transporting polypeptides 1B1 and 1B3 in ovarian cancer cells: relevance for paclitaxel transport. Biomed Pharmacother 2011, 65(6):417–426. [PubMed: 21719246]
7. Zeller C, Dai W, Steele NL, Siddiq A, Walley AJ, Wilhelm-Benartzi CS, Rizzo S, van der Zee A, Plumb JA, Brown R: Candidate DNA methylation drivers of acquired cisplatin resistance in ovarian cancer identified by methylome and expression profiling. Oncogene 2012, 31(42):4567–4576. [PubMed: 22249249]
8. Ibrahim N, He L, Leong CO, Xing D, Karlan BY, Swisher EM, Rueda BR, Orsulic S, Ellisen LW: BRCA1-associated epigenetic regulation of p73 mediates an effector pathway for chemosensitivity in ovarian carcinoma. Cancer Res 2010, 70(18):71557165.
9. Yang H, Kong W, He L, Zhao JJ, O'Donnell JD, Wang J, Wenham RM, Coppola D, Kruk PA, Nicosia SV et al.: MicroRNA expression profiling in human ovarian cancer: mi-R214 induces cell survival and cisplatin resistance by targeting PTEN. Cancer Res 2008, 68(2):425–433. [PubMed: 18199536]
10. Ye G, Fu G, Cui S, Zhao S, Bernaudo S, Bai Y, Ding Y, Zhang Y, Yang BB, Peng C: MicroRNA 376c enhances ovarian cancer cell survival by targeting activin receptor-like kinase 7: implications for chemoresistance. J Cell Sci 2011, 124(Pt 3):359–368. [PubMed: 21224400]
11. O'Connor PM, Jackman J, Bae I, Myers TG, Fan S, Mutoh M, Scudiero DA, Monks A, Sausville EA, Weinstein JN et al.: Characterization of the p53 tumor suppressor pathway in cell lines of the National Cancer Institute anticancer drug screen and correlations with the growth-inhibitory potency of 123 anticancer agents. Cancer Res 1997, 57(19):4285–4300. [PubMed: 9331090]
12. Wong KK, Izaguirre DI, Kwan SY, King ER, Deavers MT, Sood AK, Mok SC, Gershenson DM: Poor survival with wild-type TP53 ovarian cancer? Gynecol Oncol 2013, 130(3):565–569. [PubMed: 23800698]
13. Yan X, Fraser M, Qiu Q, Tsang BK: Over-expression of PTEN sensitizes human ovarian cancer cells to cisplatin-induced apoptosis in a p53-dependent manner. Gynecol Oncol 2006, 102(2):348–355. [PubMed: 16545436]
14. Ying H, Qu D, Liu C, Ying T, Lv J, Jin S, Xu H: Chemoresistance is associated with Beclin-1 and PTEN expression in epithelial ovarian cancers. Oncol Lett 2015, 9(4):1759–1763. [PubMed: 25789037]
15. Dumontet C, Sikic BI: Mechanisms of action of and resistance to antitubulin agents: microtubule dynamics, drug transport, and cell death. J Clin Oncol 1999, 17(3):1061–1070. [PubMed: 10071301]
16. Mineta K, Yamamoto Y, Yamazaki Y, Tanaka H, Tada Y, Saito K, Tamura A, Igarashi M, Endo T, Takeuchi K et al.: Predicted expansion of the claudin multigene family. FEBS Lett 2011, 585(4):606–612. [PubMed: 21276448]

17. Van Itallie C, Rahner C, Anderson JM: Regulated expression of claudin-4 decreases paracellular conductance through a selective decrease in sodium permeability. The Journal of clinical investigation 2001, 107(10):1319–1327. [PubMed: 11375422]

18. Hou J, Gomes AS, Paul DL, Goodenough DA: Study of claudin function by RNA interference. The Journal of biological chemistry 2006, 281(47):36117–36123. [PubMed: 17018523]

19. Hou J, Renigunta A, Yang J, Waldegger S: Claudin-4 forms paracellular chloride channel in the kidney and requires claudin-8 for tight junction localization. Proc Natl Acad Sci U S A 2010, 107(42):18010–18015. [PubMed: 20921420]

20. Rahner C, Mitic LL, Anderson JM: Heterogeneity in expression and subcellular localization of claudins 2, 3, 4, and 5 in the rat liver, pancreas, and gut. Gastroenterology 2001, 120(2):411–422. [PubMed: 11159882]

21. Jakab C, Halasz J, Szasz AM, Ba™unkh E, Kiss A, Schaff Z, Rusvai M, Galfi P, Kulka J: Expression and localisation of claudin-1, −2, −3, −4, −5, −7 and −10 proteins in the normal canine mammary gland. Acta Vet Hung 2008, 56(3):341–352. [PubMed: 18828486]

22. Garcia-Godinez A, Contreras RG, Gonzalez-Del-Pliego M, Aguirre-Benitez E, AcunaMacias I, de la Vega MT, Martin-Tapia D, Solano-Agama C, Mendoza-Garrido ME: Anterior and intermediate pituitary tissues express claudin 4 in follicle stellate cells and claudins 2 and 5 in endothelial cells. Cell Tissue Res 2014, 357(1):309321.

23. Kage H, Flodby P, Gao D, Kim YH, Marconett CN, DeMaio L, Kim KJ, Crandall ED, Borok Z: Claudin 4 knockout mice: normal physiological phenotype with increased susceptibility to lung injury. American journal of physiology Lung cellular and molecular physiology 2014, 307(7):L524–536. [PubMed: 25106430]

24. Stewart JJ, White JT, Yan X, Collins S, Drescher CW, Urban ND, Hood L, Lin B: Proteins associated with Cisplatin resistance in ovarian cancer cells identified by quantitative proteomic technology and integrated with mRNA expression levels. Mol Cell Proteomics 2006, 5(3):433–443. [PubMed: 16319398]

25. Casagrande F, Cocco E, Bellone S, Richter CE, Bellone M, Todeschini P, Siegel E, Varughese J, Arin-Silasi D, Azodi M et al.: Eradication of chemotherapy-resistant CD44+ human ovarian cancer stem cells in mice by intraperitoneal administration of clostridium perfringens enterotoxin. Cancer 2011.

26. Yin G, Alvero AB, Craveiro V, Holmberg JC, Fu HH, Montagna MK, Yang Y, ChefetzMenaker I, Nuti S, Rossi M et al.: Constitutive proteasomal degradation of TWIST-1 in epithelial-ovarian cancer stem cells impacts differentiation and metastatic potential. Oncogene 2013, 32(1):39–49. [PubMed: 22349827]

27. Baumgartner HK, Beeman N, Hodges RS, Neville MC: A d-Peptide Analog of the Second Extracellular Loop of Claudin-3 and −4 Leads to MisLocalized Claudin and Cellular Apoptosis in Mammary Epithelial Cells. Chem Biol Drug Des 2011, 77(2):124–136. [PubMed: 21266016]

28. Hicks DA, Galimanis CE, Webb PG, Spillman MA, Behbakht K, Neville MC, Baumgartner HK: Claudin-4 activity in ovarian tumor cell apoptosis resistance and migration. BMC Cancer 2016, 16(1):788. [PubMed: 27724921]

29. Korch C, Spillman MA, Jackson TA, Jacobsen BM, Murphy SK, Lessey BA, Jordan VC, Bradford AP: DNA profiling analysis of endometrial and ovarian cell lines reveals misidentification, redundancy and contamination. Gynecol Oncol 2012, 127(1):241248.

30. Domcke S, Sinha R, Levine DA, Sander C, Schultz N: Evaluating cell lines as tumour models by comparison of genomic profiles. Nat Commun 2013, 4:2126. [PubMed: 23839242]

31. Gao Z, Xu X, McClane B, Zeng Q, Litkouhi B, Welch WR, Berkowitz RS, Mok SC, Garner EI: C Terminus of Clostridium perfringens Enterotoxin Downregulates CLDN4 and Sensitizes Ovarian Cancer Cells to Taxol and Carboplatin. Clin Cancer Res 2011, 17(5):1065–1074. [PubMed: 21123456]

32. Agarwal R, D'Souza T, Morin PJ: Claudin-3 and claudin-4 expression in ovarian epithelial cells enhances invasion and is associated with increased matrix metalloproteinase-2 activity. Cancer Res 2005, 65(16):7378–7385. [PubMed: 16103090]

33. Ma X, Miao H, Jing B, Pan Q, Zhang H, Chen Y, Zhang D, Liang Z, Wen Z, Li M: Claudin-4 controls the proliferation, apoptosis, migration and in vivo growth of MCF-7 breast cancer cells. Oncol Rep 2015, 34(2):681–690. [PubMed: 26058359]

34. Fredriksson K, Van Itallie CM, Aponte A, Gucek M, Tietgens AJ, Anderson JM: Proteomic analysis of proteins surrounding occludin and claudin-4 reveals their proximity to signaling and trafficking networks. PloS one 2015, 10(3):e0117074. [PubMed: 25789658]

35. McGrail DJ, Khambhati NN, Qi MX, Patel KS, Ravikumar N, Brandenburg CP, Dawson MR: Alterations in ovarian cancer cell adhesion drive taxol resistance by increasing microtubule dynamics in a FAK-dependent manner. Sci Rep 2015, 5:9529. [PubMed: 25886093]

36. Mok SC, Bonome T, Vathipadiekal V, Bell A, Johnson ME, Wong KK, Park DC, Hao K, Yip DK, Donninger H et al.: A gene signature predictive for outcome in advanced ovarian cancer identifies a survival factor: microfibril-associated glycoprotein 2. Cancer Cell 2009, 16(6):521–532. [PubMed: 19962670]

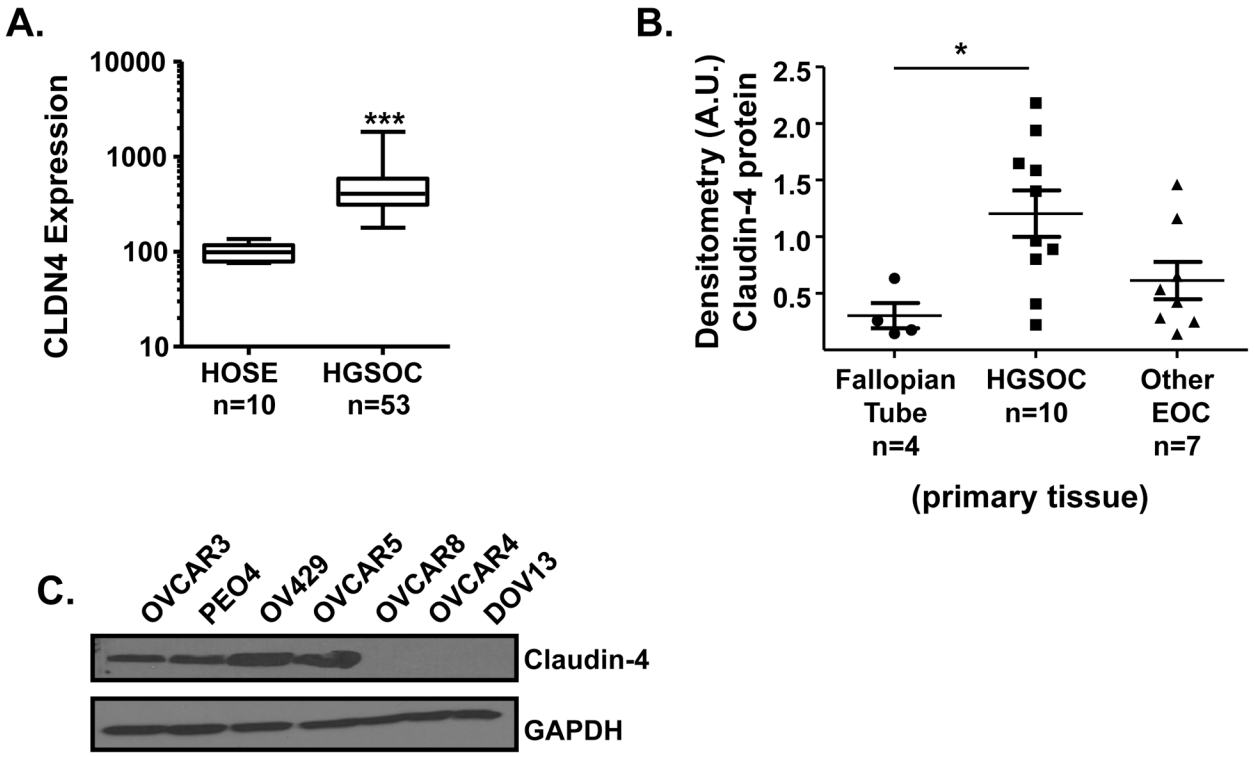

Figure 1: Claudin-4 expression in high grade serous ovarian cancer cells.

(**A**) CLDN4 gene expression levels in laser capture microdissected specimens of human high grade serous ovarian tumors compared to isolated normal human ovarian surface epithelial cells [36]. Western blot analysis of claudin-4 protein levels in human patient samples of normal fallopian tube and ovarian cancer (**B**) as well as high grade serous ovarian tumor cell lines (**C**), using GAPDH as a loading control. Mean ± s.e.m., n=10 HOSE, n=10–53 HGSOC tumor specimens, n=7 other EOC subtypes, *p<0.05, ***p<0.0001.

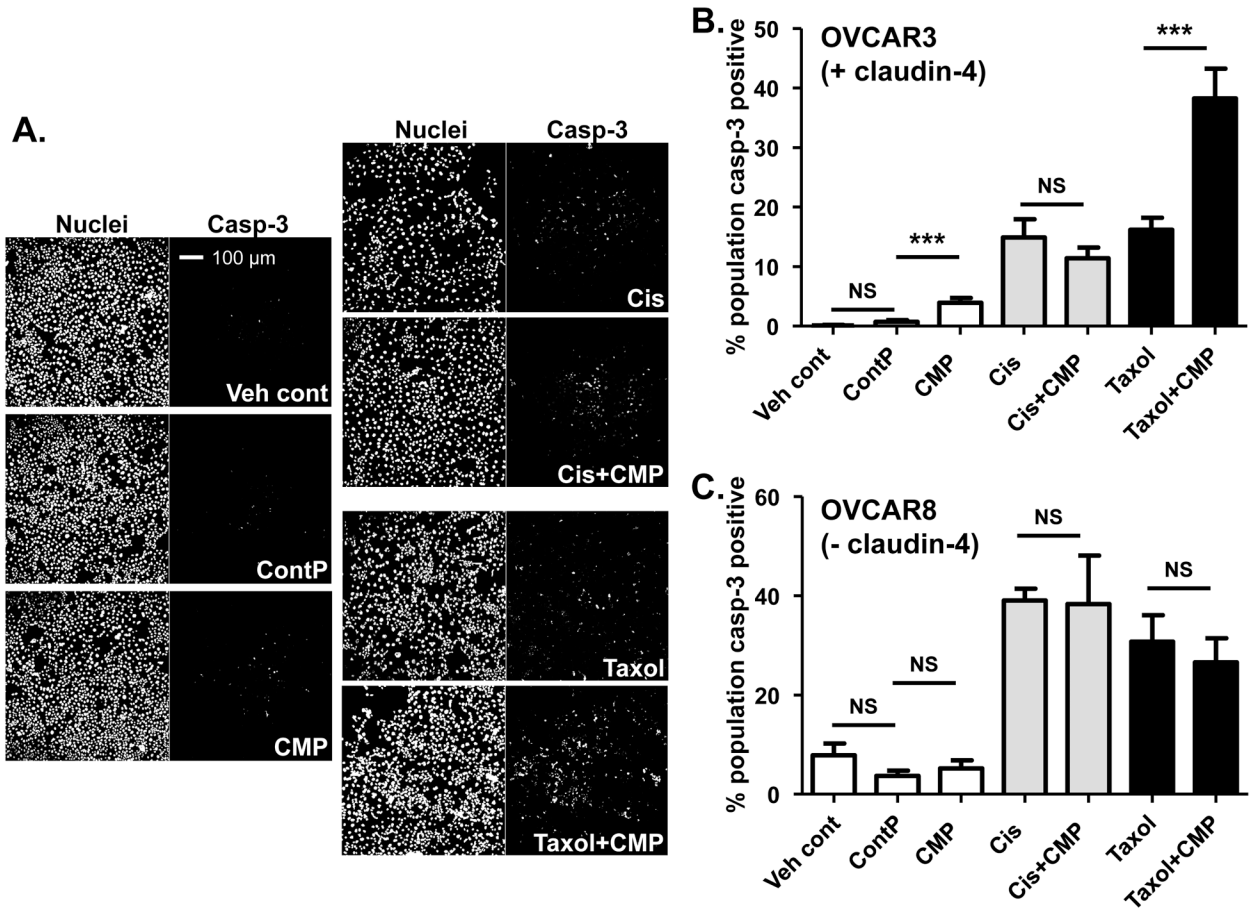

Figure 2: Disruption of claudin-4 activity with CMP enhances paclitaxel response.

Representative images of nuclei (DAPI staining) and activated caspase-3 (fluorescent antibody directed to cleaved caspase-3) from OVCAR3 cells (**A**). Quantification of caspase-3 activation in OVCAR3 (**B**) and OVCAR8 (**C**) cells treated for 24 hours with vehicle control (Veh cont), 400 µM inactive control peptide (ContP), 400 µM CMP, 10 µM Cisplatin (Cis), CMP + Cisplatin, 10 nM paclitaxel (taxol), or CMP + paclitaxel. Percent of cell population positive for caspase-3 activation was calculated using SlideBook software (3i). Mean ± s.e.m., n=3, NS=not significant, ***$p<0.001$ *vs.* control/drug only.

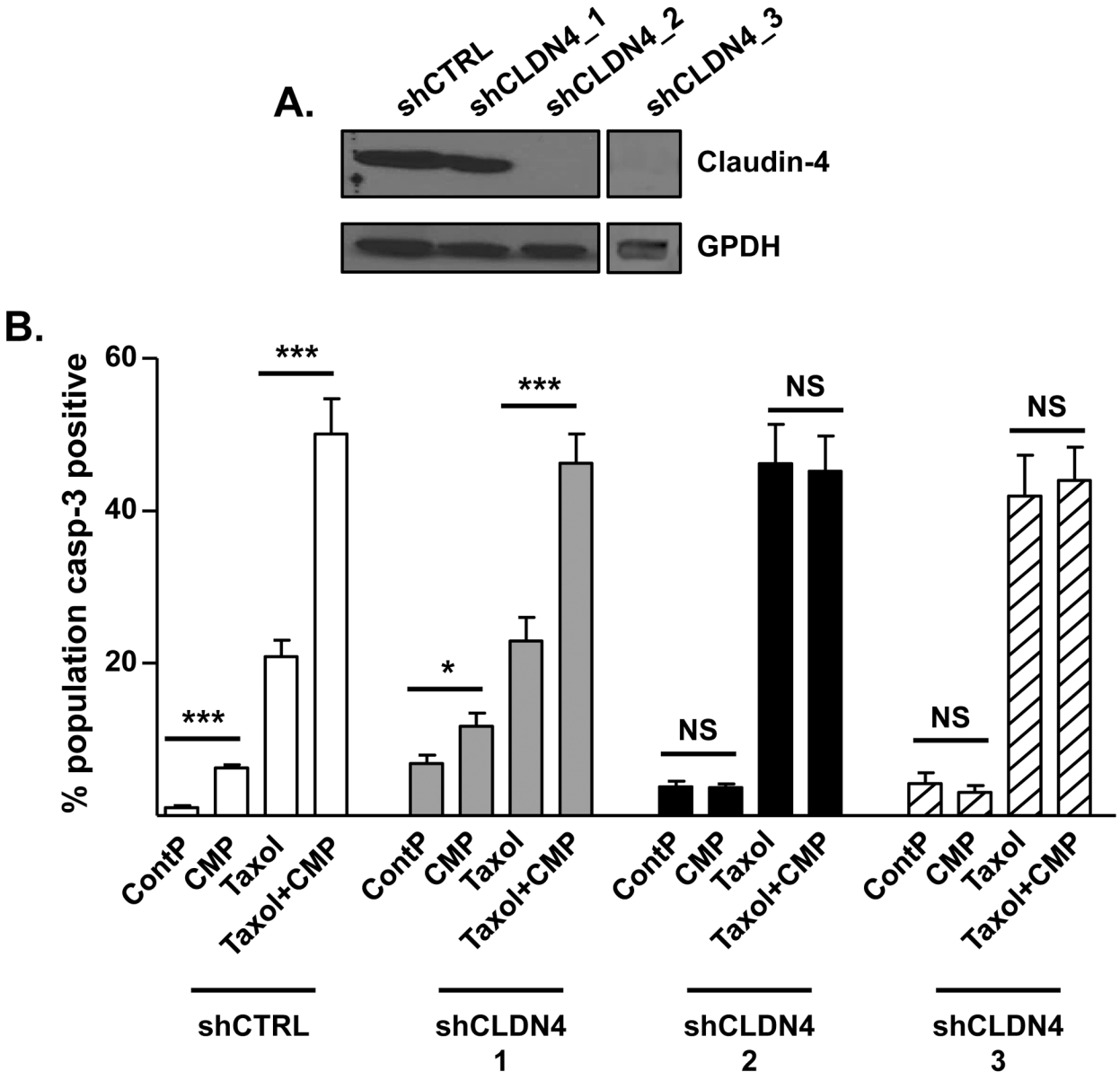

Figure 3: Loss of claudin-4 expression enhances paclitaxel response.

(**A**) Western blot analysis of claudin-4 protein in OVCAR3 cells treated with control empty vector shRNA (shCTRL) or claudin-4-targeted shRNA (shCLDN4_1, shCLDN4_2, shCLDN4_3). GAPDH was used as a loading control. (**B**) Immunofluorescence analysis of cells treated with 400 μM inactive control peptide (ContP), 400 μM CMP, 10 nM paclitaxel (taxol), or CMP + paclitaxel for 24 hours. Cells were treated with fluorescent antibody directed to cleaved caspase-3 and DAPI (nuclei) and percent of cell population positive for caspase-3 was calculated using SlideBook software (3i). Mean ± s.e.m., n=3 per treatment group, NS=not significant, *$p<0.05$, ***$p<0.001$ *vs.* control/paclitaxel only.

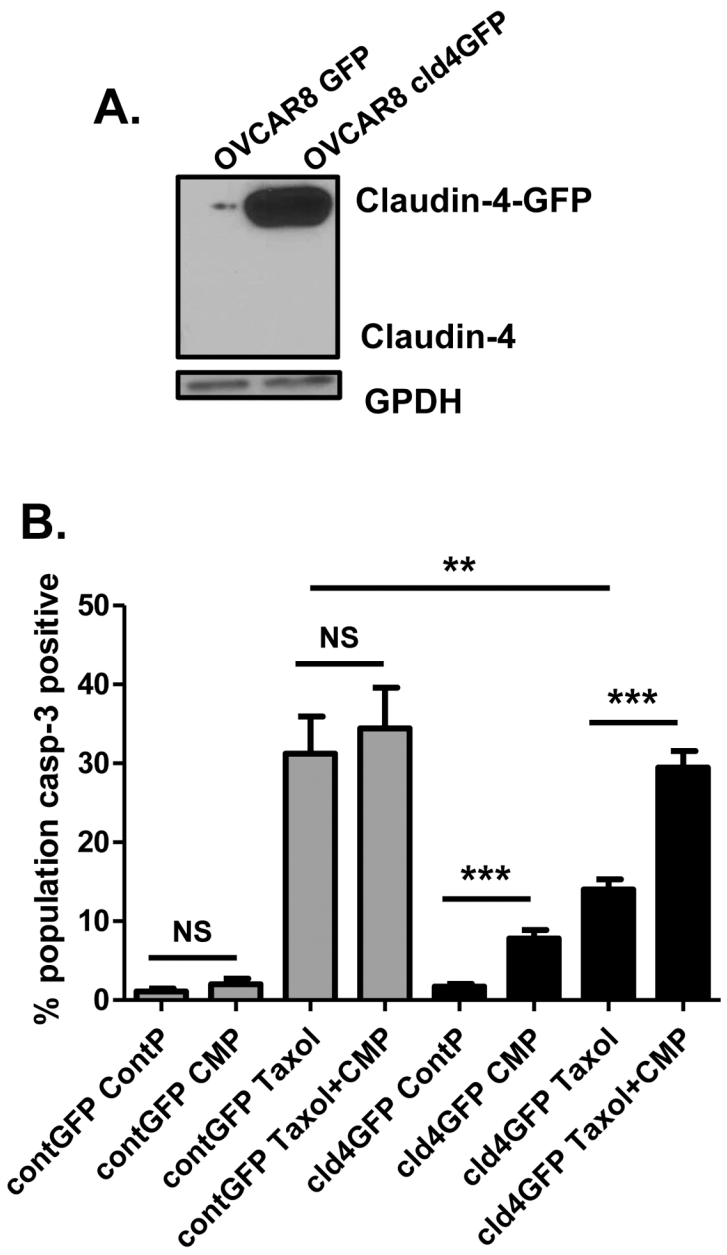

Figure 4: Overexpression of claudin-4 reduces paclitaxel response.

(**A**) Western blot analysis of claudin-4 protein in OVCAR8 cells transduced with GFP only or claudin-4-GFP. GAPDH was used as a loading control. (**B**) Immunofluorescence analysis of fixed OVCAR8 cells that were treated with 400 μM inactive control peptide (ContP), 400 μM CMP, 10 nM paclitaxel (taxol), or CMP + paclitaxel for 24 hours. Cells were treated with fluorescent antibody directed to cleaved caspase-3 and DAPI (nuclei) and percent of cell population positive for caspase-3 was calculated using SlideBook software (3i). Mean ± s.e.m., n=3 per treatment group, NS=not significant, ** $p<0.01$, *** $p<0.001$ *vs.* control/ paclitaxel only.

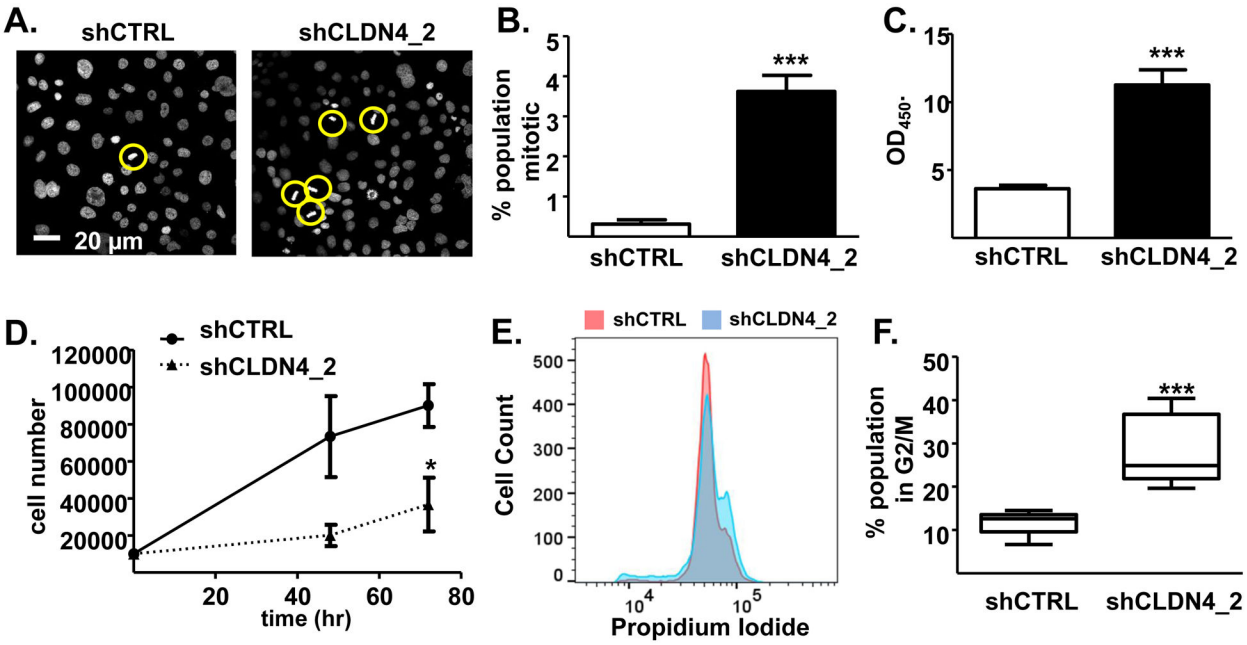

Figure 5: Loss of claudin-4 leads to delayed mitotic progression.

(**A**) Representative images of DAPI (DNA) staining in fixed monolayers of control knockdown (shCTRL) and claudin-4 knockdown (shCLDN4_2) OVCAR3 cells. Yellow circles highlight mitotic figures. (**B**) Visual counting of mitotic figures from DAPI images and (**C**) colorimetric measurement of phosphorylated H2B (mitotic marker) to quantify population of mitotic cells in shCTRL (white bars) and shCLDN4_2 (black bars) OVCAR3 cells. (**D**) Proliferation rates of shCTRL (circles/solid line) and shCLDN4_2 (triangles/dotted line) OVCAR3 cells. (**E**) Representative histograms of propidium iodide staining six hours after release from serum starvation synchronization in shCTRL and shCLDN4_2 cells. (**F**) Quantification of the percent of the total cell population in the G2/M phase of the cell cycle using FlowJo software. Mean±sem, n=3, *p<0.05, ****p*<0.001 *vs.* control/paclitaxel only.

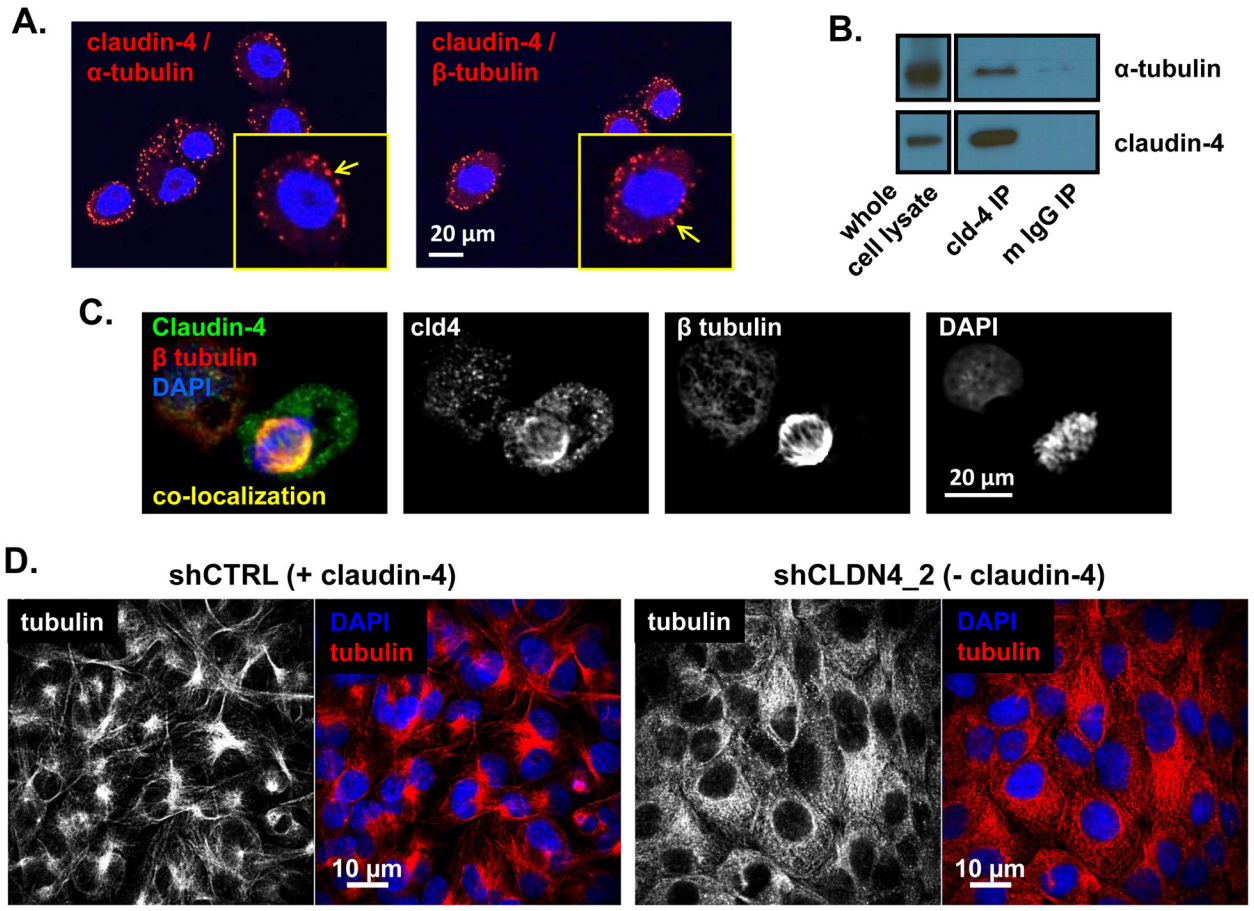

Figure 6: Claudin-4 interacts with tubulin.

(**A**) Proximity ligation assay using antibodies directed at claudin-4 and α-tubulin or β-tubulin. Red fluorescence indicates protein-protein interaction. Yellow outlined boxes are higher magnification of cell from image. Arrows point to sites of protein-protein interaction. (**B**) Immunoprecipitation (IP) of claudin-4 (cld-4 IP) and IgG (mouse IgG IP) from OVCAR3 lysates blotted for presence of α-tubulin and claudin-4. (**C**) Immunofluorescence of claudin-4 (green) and β-tubulin (red), with DAPI (blue), in mitotic OVCAR3 cell. Yellow color indicates co-localization of claudin-4 and β-tubulin. (**D**) Immunofluorescence of microtubules (β-tubulin; white/red) and nuclei (DAPI/blue) in cells expressing (shCTRL) and not expressing (shCLDN4_2) claudin-4.

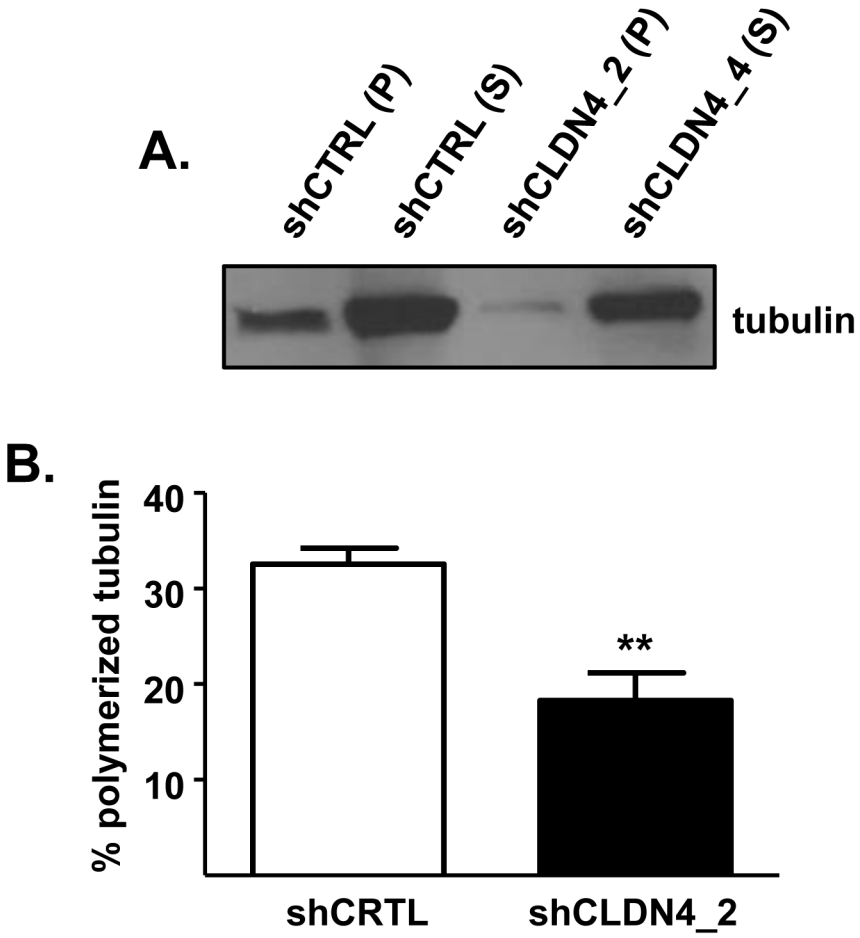

Figure 7: Claudin-4 alters tubulin polymerization.

(**A**) Representative Western blot analysis of polymerized (P, pellet fraction) and non-polymerized (S, supernatant fraction) tubulin levels in OVCAR3 cells expressing claudin-4 (shCTRL) and cells with claudin-4 expression silenced (shCLDN4_2). (**B**) Quantification of the percent of the total tubulin that is polymerized. Mean±sem, n=4, **p<0.01.